Structural Engineering and Mechanics, Vol. 6, No. 7 (1998) 727-746
DOI: http://dx.doi.org/10.12989/sem.1998.6.7.727

Analysis of composite plates using various plate theories Part 2: Finite element model and numerical results

P. Bose† and J.N. Reddy‡

Department of Mechanical Engineering, Texas A&M University, College Station, TX 77843-3123, U.S.A.

Abstract. Finite element models and numerical results are presented for bending and natural vibration using the unified third-order plate theory developed in Part 1 of this paper. The unified third-order theory contains the classical, first-order, and other third-order plate theories as special cases. Analytical solutions are developed using the Navier and Lévy solution procedures (see Part 1 of the paper). Displacement finite element models of the unified third-order theory are developed herein. The finite elelment models are based on C^0 interpolation of the inplane displacements and rotation functions and C^1 interpolation of the transverse deflection. Numerical results of bending and natural vibration are presented to evaluate the accuracy of various plate theories.

Key words: finite element model; anaytical solutions; bending; vibration; shear deformation; third-order theory.

1. Introduction

In the first part of this paper we developed a unified third-order laminate plate theory that contains classical, first order and other third order theories as special cases. Analytical solutions using the Navier and Lévy solution procedures were presented. Though the analytical solutions are useful for the purpose of comparison, their scope is limited to particular geometries, loads, and boundary conditions. The Navier solutions are limited to simply supported rectangular plates and the Lévy solutions are for rectangular plates with two parallel edges simply supported and the other two having arbitrary combination of simply supported, free, and clamped boundary conditions. For a more general treatment of complex problems, one has to turn to an approximate numerical method, such as the finite element method. In this paper, we develop finite element models of the different laminated plate theories. Numerical results of bending and vibration for a number of problems are discussed in this paper.

† Research Assistant
‡ University Distinguished Professor

2. Finite element models

2.1. Weak form

Consider the equilibrium equations of the general third order theory (Bose and Reddy 1997). For each of the equations, we construct weighted-integral form by multiply the entire equation by a weight function φ and integrating it over the domain Ω^e of a typical element. For the i-th equation, this will look like

$$0 = \int_{\Omega^e} \varphi_i [\text{RHS of modified equation } i] \, dxdy \tag{1}$$

The above statement is called the *weighted-integral* statement equivalent to the original (Reddy 1993). Next Eq. (1) is integrated by parts to weaken the continuity requirement on the approximation functions used for the unkown displacements. The weighted-integral statement so obtained is called the *weak form* (see Reddy 1993, 1997).

From weak forms (not given here) of the theories considered here, it is easy to identify the primary and secondary variables by examining the boundary terms. The specification of the primary variables constitute the essential (or geometric) boundary conditions while the specification of the secondary variables constitute the natural (or force) boundary conditions. The essential and natural boundary conditions of the two theories are as follows:

General third order theory (GTOT)

$$\begin{aligned} &\text{essential:} \quad \text{specify} \quad u_n, u_s, w, \phi_n, \phi_s, \psi_n, \psi_s, \psi_z, \theta_n, \theta_s, \theta_z \\ &\text{natural:} \quad \text{specify} \quad N_n, N_{ns}, N_z, M_n, M_{ns}, P_n, P_{ns}, M_z, S_n, S_{ns}, P_z \end{aligned} \tag{2}$$

General third order theory of Reddy (GTTR)

$$\begin{aligned} &\text{essential:} \quad \text{specify} \quad u_n, u_s, w, \phi_n, \phi_s, \psi_3, \frac{\partial \psi_3}{\partial n}, \frac{\partial \psi_3}{\partial s}, \zeta, \frac{\partial \zeta}{\partial n}, \frac{\partial \zeta}{\partial s} \\ &\text{natural:} \quad \text{specify} \quad N_n, N_{ns}, N_z, M_n, M_{ns}, Q_z, P_n, P_{ns}, R_z, S_n, S_{ns} \end{aligned} \tag{3}$$

2.2. Finite element models

In the finite element method, the primary variables are approximated as continuous variables throughout the domain, including interelement boundaries. The list of primary variables of the general third order theory show that all generalized displacements of the theory, and not their derivatives, must be carried (C^0-continuity) as the nodal variables to satisfy the continuity requirement. For the special third order theory, the first derivatives of some primary variables also need to be continuous across the elements. Hence the nodal degrees of freedom should include these first derivatives, i.e., C^1 continuity of the element is required. This is true for three of the special cases of the special third order theory, GTTR, STTR, and CLPT. For FSDT, however, C^0 continuity is enough.

The nodal degrees of freedom used for the different theories are given below.

CLPT: $u, v, w, \partial w/\partial x, \partial w/\partial y, \partial^2 w/\partial x \partial y$

FSDT: u, v, w, ϕ_1, ϕ_2

STTR: $u, v, w, \partial w/\partial x, \partial w/\partial y, \partial^2 w/\partial x \partial y, \phi_1, \phi_2$

GTTR: $u, v, w, \phi_1, \phi_2, \psi_3, \partial\psi_3/\partial x, \partial\psi_3/\partial y, \partial^2\psi_3/\partial x\partial y, \zeta, \partial\zeta/\partial x, \partial\zeta/\partial y, \partial^2\zeta/\partial x\partial y$

GTOT: $u, v, w, \phi_1, \phi_2, \psi_1, \psi_2, \psi_3, \theta_1, \theta_2, \theta_3$ (4)

All the generalized displacements in GTOT and u, v, ϕ_1, ϕ_2 in the other theories (also w in GTTR) can be interpolated by the Lagrange or serendipity family of interpolation functions. That is

$$\Delta(x, y, t) = \sum_{j=1}^{n} \Delta_j(t)\psi_j(x, y) \tag{5}$$

where Δ can be any of the above-mentioned displacements, Δ_j are the nodal values of Δ, and ψ_j are the interpolation functions. The value of n can be four for linear Lagrange element, eight for eight-node serendipity element, or nine for quadratic Lagrange element.

The variables w (in the case of CLPT and STTR) and ψ_3 and ζ in the case of GTTR are interpolated by Hermite cubic interpolation functions. The cross derivative term is also taken as a nodal degree of freedom. Such an element is called a *conforming* element (Reddy 1993). If $\bar{\Delta}$ represents any of the displacements mentioned above then

$$\bar{\Delta}(x, y, t) = \sum_{j=1}^{m} \bar{\Delta}_j(t)\hat{\phi}_j(x, y) \tag{6}$$

$\bar{\Delta}_j$ are the nodal values of $\bar{\Delta}$, and $\hat{\phi}_j$ are the Hermite cubic interpolation functions. For a four-node element, there will be four degrees of freedom at each node thus making the value of m to be 16.

For the finite element model, the weak forms are first written out explicitly in terms of the generalized displacements. Then we substitute the interpolation functions for the generalized displacements in the weak form. The weight functions φ_i for each of the equations are substituted by the corresponding interpolation functions (ψ_i or $\hat{\phi}_i$). This leads to a set of algebraic equations for each element, the i-th equation of which is given by

$$\sum_{\beta=1}^{p}\sum_{j=1}^{n(\beta)} (K_{ij}^{\alpha\beta}\Delta_j^{\beta} + M_{ij}^{\alpha\beta}\ddot{\Delta}_j^{\beta}) = f_i^{\alpha} + Q_i^{\alpha} \qquad i = 1, 2, ..., n(\alpha) \tag{7}$$

where α=1, 2, ···, p. The value of p is 11 for the general third order theory, and 7 for the special third order theory. It represents the number of primary variables in the problem. The element stiffness matrix $[K]$ and element mass matrix $[M]$ each have $p \times p$ submatrices. The size of a submatrix $[K^{\alpha\beta}]$ or $[M^{\alpha\beta}]$ is $n(\alpha) \times n(\beta)$. $n(\alpha)$=$n(\beta)$=4 or 8 or 9, depending on whether the corresponding primary variable is interpolated by linear Lagrange functions, serendipity functions or quadratic Lagrange functions. $n(\alpha)$=$n(\beta)$=16, if the corresponding primary variable is interpolated by Hermite cubic interpolation functions. The element force vector $\{f\}$ and the vector of secondary variables $\{Q\}$ have p subvectors, one corresponding to each primary variable. The size of each subvector is $n(\alpha) \times 1$. In matrix notation, the system of finite element equations for each element can be written as

$$[K^e]\{\Delta_e\} + [M^e]\{\ddot{\Delta}^e\} = \{f^e\} + \{Q^e\} \tag{8}$$

The elements of the mass and stiffness matrices are given explicitly in Bose (1995) and Reddy (1997).

Table 1 Material properties

Aragonite	C_{11}	23.2×10^6 psi
	C_{12}	5.41×10^6 psi
	C_{13}	0.25×10^6 psi
	C_{22}	12.6×10^6 psi
	C_{23}	2.28×10^6 psi
	C_{33}	12.3×10^6 psi
	C_{44}	6.19×10^6 psi
	C_{55}	3.71×10^6 psi
	C_{66}	6.10×10^6 psi
Graphite-epoxy	E_1	19.2×10^6 psi
	E_2	1.56×10^6 psi
	E_3	1.56×10^6 psi
	G_{23}	0.523×10^6 psi
	G_{13}	0.82×10^6 psi
	G_{12}	0.82×10^6 psi
	ν_{23}	0.49
	ν_{13}	0.24
	ν_{12}	0.24
Material 3	E_1	variable
	E_2	1.0×10^6 ps
	E_3	1.0×10^6 psi
	G_{23}	0.5×10^6 psi
	G_{13}	0.6×10^6 psi
	G_{12}	0.6×10^6 psi
	ν_{23}	0.25
	ν_{13}	0.25
	ν_{12}	0.25

3. Results and disscussion

3.1. Introduction

Three computer programs were written to solve a number of bending and free vibration problems in laminated plates. The first program was for finding the solution by Navier's method, the second for finding the solution by Lévy's method, and the third was a finite element program for the analysis of a general laminated composite plate problem for arbitrary loadings, geometries, and boundary conditions.

3.1.1. Material properties

Three different materials were used for the numerical examples. Their properties are listed in Table 1. The first material is Aragonite. Exact solutions for a number of cases were given for this material by Srinivas *et al.* (1966, 1970, 1973). Results obtained from the different theories have been compared with these exact solutions. The second material is graphite/epoxy. The majority of numerical results given in this paper are for this material. Noor (1989)

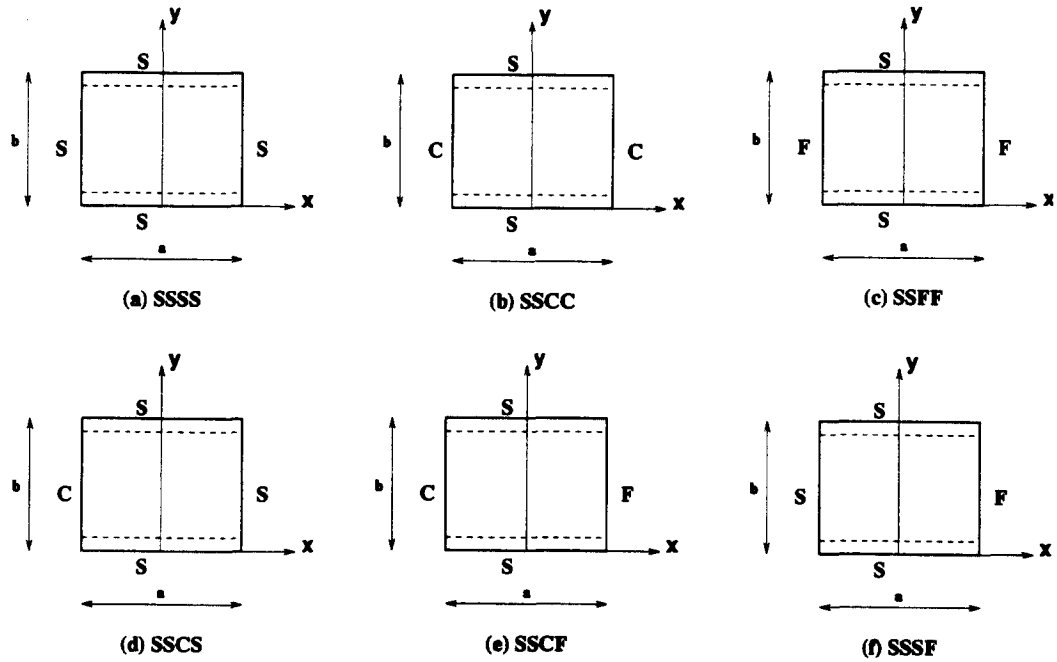

Fig. 1 Boundary conditions for Lévy solution

gave exact solutions to free vibration problems for a high modulus composite, which we shall call Material 3. We compare results of free vibration from the different theories with the exact solutions given by Noor.

3.1.2. Analytical solutions

The theoretical basis for The Navier and Lévy solutions have been explained in Bose (1995) and Reddy (1997). In both these methods, the solutions are approximated in the form of an infinite series which is truncated after a few terms. For the Navier method, m=n=25 gives sufficiently accurate results. In the Lévy method, the convergence is extremely fast as mentioned in the concluding part of Part 1. Taking only the first four terms gives very good results in all the cases. For problems which have been solved by the Navier method, all four sides of the plate are simply-supported, and the remaining two edges can have any combination of free, clamped, or simply-supported boundary conditions. The different sets of boundary conditions for which results have been obtained are shown in Fig. 1. For example, the acronym SSCF refers to a plate which is simply-supported y=0 and y=b, clamped at x= − a/2, and free at x=+a/2. A total of six such boundary conditions have been investigated.

3.1.3. Finite element solutions

The different boundary conditions used, including the symmetry boundary conditions, on the primary variables (PV's) are shown in tabular form for the different theories in Tables 2-6. Symm_X refers to symmetry boundary conditions along line parallel to the x-axis. Symm_Y, refers to simply-supported boundary conditions along edges parallel to the y=axis.

Table 2 Boundary conditions for CLPT

	Specified primary variables
Symm_X	$v=\partial w/\partial y=\partial^2 w/\partial x\partial y=0$
Symm_Y	$u=\partial w/\partial x=\partial^2 w/\partial x\partial y=0$
Simple_X	$u=w=\partial w/\partial x=0$
Simple_Y	$v=w=\partial w/\partial y=0$
Clamped_X	All PVs specified zero
Free_X	No PVs specified

Table 3 Boundary conditions for FSDT

	Specified primary variables
Symm_X	$v=\phi_2=0$
Symm_Y	$u=\phi_1=0$
Simple_X	$u=w=\phi_1=0$
Simple_Y	$v=w=\phi_2=0$
Clamped_X	All PVs specified zero
Free_X	No PVs specified

Table 4 Boundary conditions for STTR

	Specified primary variables
Symm_X	$v=\partial w/\partial y=\partial^2 w/\partial x\partial y=\phi_2=0$
Symm_Y	$u=\partial w/\partial x=\partial^2 w/\partial x\partial y=\phi_1=0$
Simple_X	$u=w=\partial w/\partial x=\phi_1=0$
Simple_Y	$v=w=\partial w/\partial y=\phi_2=0$
Clamped_X	All PVs specified zero
Free_X	No PVs specified

Table 5 Boundary conditions for GTTR

	Specified primary variables
Symm_X	$v=\phi_2=\partial\psi_3/\partial y=\partial^2\psi_3/\partial x\partial y=\partial\zeta/\partial y=\partial^2\zeta/\partial x\partial y=0$
Symm_Y	$u=\phi_1=\partial\psi_3/\partial x=\partial^2\psi_3/\partial x\partial y=\partial\zeta/\partial x=\partial^2\zeta/\partial x\partial y=0$
Simple_X	$u=w=\phi_1=\psi_3=\partial\psi_3/\partial x=\zeta=\partial\zeta/\partial x=0$
Simple_Y	$v=w=\phi_2=\psi_3=\partial\psi_3/\partial y=\zeta=\partial\zeta/\partial y=0$
Clamped_X	All PVs specified zero
Free_X	No PVs specified

Table 6 Boundary conditions for GTOT

	Specified primary variables
Symm_X	$v=\phi_2=\psi_2=\theta_2=0$
Symm_Y	$u=\phi_1=\psi_1=\theta_1=0$
Simple_X	$u=w=\phi_1=\psi_1=\psi_3=\theta_1=\theta_3=0$
Simple_Y	$v=w=\phi_2=\psi_2=\psi_3=\theta_2=\theta_3=0$
Clamped_X	All PVs specified zero
Free_X	No PVs specified

Table 7 Transverse deflection ($C_{11}w/hq_0$) in an orthotropic plate under uniform transverse load

b/a	h/a	$C_{11}w/hq_0$				
		Exact	GTTR	STTR	FSDT	CLPT
2	0.05	21542.0	21543.0	21544.2	21544.3	21210.6
	0.10	1408.5	1408.5	1409.0	1409.0	1325.7
	0.14	387.23	387.25	387.55	387.60	345.08
1	0.05	10443.0	10443.6	10446.8	10446.8	10250.7
	0.10	688.57	688.60	689.54	689.57	640.67
	0.14	191.07	191.09	191.61	191.64	166.77
0.5	0.05	2048.7	2048.8	2051.5	2051.5	1989.0
	0.10	139.08	139.09	139.83	139.85	124.31
	0.14	39.790	39.801	40.215	40.231	32.359

Table 8 Normal stress (σ_x/q_0) in an orthotropic plate under uniform transverse load

b/a	h/a	σ_x/q_0				
		Exact	GTTR	STTR	FSDT	CLPT
2	0.05	262.67	262.67	262.67	262.08	262.26
	0.10	65.975	65.977	65.978	65.392	65.564
	0.14	33.862	33.864	33.865	33.279	33.451
1	0.05	144.31	144.31	144.32	143.91	144.39
	0.10	36.021	36.024	36.034	35.623	36.098
	0.14	18.346	18.348	18.358	17.948	18.417
0.5	0.05	40.657	40.658	40.708	40.525	40.860
	0.10	10.025	10.026	10.074	9.893	10.215
	0.14	5.0364	5.0389	5.0842	4.9052	5.2118

Table 9 Normal stress (σ_y/q_0) in an orthotropic plate under uniform transverse load

b/a	h/a	σ_y/q_0				
		Exact	GTTR	STTR	FSDT	CLPT
2	0.05	79.545	79.558	79.337	79.230	79.119
	0.10	20.204	20.221	20.038	19.891	19.780
	0.14	10.515	10.534	10.350	10.203	10.092
1	0.05	87.080	87.100	86.990	86.826	86.486
	0.10	22.210	22.232	22.123	21.959	21.622
	0.14	11.615	11.637	11.529	11.365	11.031
0.5	0.05	54.279	54.303	54.284	54.097	53.838
	0.10	13.888	13.912	13.895	13.708	13.460
	0.14	7.2794	7.3055	7.2909	7.1038	6.8671

Table 10 Shear stresses (τ_{xz}/q_0) in an orthotropic plate under uniform transverse load

b/a	h/a	$-\tau_{xz}/q_0$				
		Exact	GTTR	STTR	FSDT	CLPT
2	0.05	14.048	14.149	14.187	11.411	0
	0.10	6.9266	6.9852	7.0290	5.7032	0
	0.14	4.8782	4.9368	4.9816	4.0716	0
1	0.05	10.873	11.009	11.048	8.8999	0
	0.10	5.3411	5.3987	5.4462	4.4367	0
	0.14	3.7313	3.7882	3.8383	3.1566	0
0.5	0.05	6.2434	6.3098	6.3524	5.1430	0
	0.10	2.9573	3.0125	3.0676	2.5332	0
	0.14	1.9987	2.0522	2.1128	1.7749	0

Symm_Y, Simple_X, Clamped_Y and Free_Y have similar meaning. For bending analysis of SSSS, SSCC, SSFF plates, quarter-plate models have been used. For bending analysis of SSCS, SSCF, and SSSF plates, half-plate models have been used. For free vibration analysis, half-plate models have been used for all the six sets of boundary conditions. The discretization used for a quarter-plate model is a 8×8 mesh of 4-node elements for CLPT, STTR and GTTR. For FSDT and GTOT, two meshes have been used for the quarter-plate

Table 11 Transverse deflection and stresses in a three-ply laminate under uniform transverse load ($\beta=E_{x1}/E_{x2}=10$)

$\beta=E_{x1}/E_{x2}$	10				
Source	Exact	GTTR	STTR	FSDT	CLPT
$-wE_{x2}/hq_0$	159.38	154.38	154.53	136.23	118.82
σ_x/q_0					
Top ply at top surface	65.332	65.407	65.335	65.272	66.947
Top ply at interface	48.857	50.039	49.937	52.217	53.557
Mid ply at upper interface	4.9030	5.0039	4.9937	5.2217	5.3557
Mid ply at lower interface	−4.8600	−4.9740	−4.9937	−5.2217	−5.3557
Bottom ply at interface	−48.609	−49.740	−49.937	−52.217	−53.557
Bottom ply at bottom surface	−65.083	−65.107	−65.335	−65.272	−66.947
σ_y/q_0					
Top ply at top surface	43.566	43.427	43.200	41.290	40.099
Top ply at interface	33.413	33.787	33.606	33.032	32.097
Mid ply at upper interface	3.4995	3.3787	3.3606	3.3032	3.2079
Mid ply at lower interface	−3.3669	−3.3653	−3.3606	−3.3032	−3.2079
Bottom ply at interface	−33.756	−33.653	−33.606	−33.032	−32.097
Bottom ply at bottom surface	−43.098	−43.294	−43.200	−41.290	−40.099
$-\tau_{xz}/q_0$					
Mid ply at upper interface	3.9285	1.5274	1.5332	1.5785	0
Mid ply at midsurface	4.0959	4.2427	4.2589	1.5785	0
Mid ply at lower interface	3.5154	1.5274	1.5332	1.5785	0

Table 12 Comparison of the lowest natural frequency of an orthotropic square plate: $a/h=10$, $\bar{w}=wh(\rho/C_{11})^{1/2}$

m	n	Exact	GTTR	STTR	FSDT	CLPT
1	1	0.0474	0.0474	0.0474	0.0474	0.0493
1	2	0.1033	0.1033	0.1032	0.1032	0.1098
2	1	0.1188	0.1188	0.1188	0.1187	0.1327
2	2	0.1694	0.1694	0.1693	0.1692	0.1924
1	3	0.1888	0.1888	0.1884	0.1884	0.2070
3	1	0.2180	0.2181	0.2180	0.2178	0.2671
2	3	0.2475	0.2476	0.2471	0.2469	0.2879
3	2	0.2624	0.2625	0.2623	0.2619	0.3248
1	4	0.2969	0.2969	0.2960	0.2959	0.3371
4	1	0.3319	0.3320	0.3320	0.3311	0.4471
3	3	0.3320	0.3321	0.3315	0.3310	0.4172
2	4	0.3476	0.3476	0.3466	0.3463	0.4152
4	2	0.3070	0.3708	0.3706	0.3696	0.5018

Table 13 Comparison of the second lowest natural frequency of an orthotropic square plate: $a/h=10$, $\bar{w}=wh(\rho/C_{11})^{1/2}$

m	n	Exact	GTTR	STTR	FSDT
1	1	1.3077	1.3085	1.3086	1.3159
1	2	1.3331	1.3339	1.3339	1.3410
2	1	1.4205	1.4213	1.4215	1.4285
2	2	1.4316	1.4324	1.4323	1.4393
1	3	1.3765	1.3773	1.3772	1.3841
3	1	1.5777	1.5786	1.5788	1.5857
2	3	1.4596	1.4604	1.4603	1.4671
3	2	1.5651	1.5659	1.5657	1.5727
1	4	1.4372	1.4379	1.4379	1.4445
4	1	1.7179	1.7187	1.7186	1.7265
3	3	1.5737	1.5745	1.5744	1.5812
2	4	1.5068	1.5076	1.5076	1.5142
4	2	1.6940	1.6948	1.6947	1.7022

model; one a 8×8 mesh of linear Lagrange elements, and the other a 4×4 mesh of quadratic Lagrange elements (referred to in the tables as FEM_L and FEM_Q respectively). For half-plate models, the discretizations used are a 16×8 mesh of 4-node elements for all the theories. Additionally, a 8×4 mesh of 9-node quadratic Lagrange elements were used for FSDT and GTOT.

3.2. Laminate theory solutions vs. 3-D elasticity solutions

The exact solutions of different laminate theories were compared with the 3-D elasticity (exact) solutions given by Srinivas and Rao (1966, 1970) (Tables 7-14), and Noor (1989) (Tables 15 and 16) for rectangular plates. In all cases, the plate is assumed to be simply-

Table 14 Comparison of the third lowest natural frequency of an orthotropic square plate: $a/h=10$, $\bar{w}=wh(\rho/C_{11})^{1/2}$

m	n	Exact	GTTR	STTR	FSDT
1	1	1.6530	1.6542	1.6550	1.6646
1	2	1.7160	1.7178	1.7209	1.7305
2	1	1.6805	1.6818	1.6827	1.6921
2	2	1.7509	1.7528	1.7561	1.7655
1	3	1.8115	1.8143	1.8208	1.8306
3	1	1.7334	1.7347	1.7361	1.7450
2	3	1.8523	1.8552	1.8620	1.8715
3	2	1.8195	1.8215	1.8253	1.8341
1	4	1.9306	1.9349	1.9461	1.9560
4	1	1.8548	1.8564	1.8586	1.8657
3	3	1.9289	1.9320	1.9391	1.9480
2	4	1.9749	1.9793	1.9906	2.0002
4	2	1.9447	1.9469	1.9511	1.9587

supported on all four edges.

3.2.1. Bending results

Table 7 gives the transverse deflections w at the mid-point of the plate ($x/a=0.5$, $y/b=0.5$, $z/h=0$). Tables 8 and 9 give the normal stresses σ_x and σ_y respectively at the center of the top surface of the plate ($x/a=0.5$, $y/b=0.5$, $z/h=-0.5$), Table 10 gives the shear stresses τ_{xz} at the

Table 15 Effect of degree of orthotropy of individual layers on the fundamental frequency of simply-supported symmetric square laminates: $a/h=5$, $\bar{w}=10\times w(\rho h^2/E_T)^{1/2}$

Number of layers	Source	E_l/E_T				
		3	10	20	30	40
3	Exact	2.6474	3.2841	3.8241	4.1089	4.3006
	GTTR	2.6286	3.2679	3.7011	3.9456	4.1150
	STTR	2.6211	3.2604	3.6940	3.9390	4.1053
	FSDT	2.6258	3.2793	3.7110	3.9541	4.1158
	CLPT	2.9198	4.1264	5.4043	6.4336	7.3196
5	Exact	2.6587	3.4089	3.9792	4.3140	4.5374
	GTTR	2.6416	3.3802	3.9439	4.2809	4.5106
	STTR	2.6340	3.3723	3.9365	4.2743	4.5047
	FSDT	2.6337	3.3680	3.9306	4.2714	4.5068
	CLPT	2.9198	4.1264	5.4043	6.4336	7.3196
7	Exact	2.6640	3.4432	4.0547	4.4210	4.6679
	GTTR	2.6460	3.4202	4.0310	4.4008	4.6533
	STTR	2.6384	3.4125	4.0240	4.3947	4.6480
	FSDT	2.6376	3.4079	4.0147	4.3818	4.6315
	CLPT	2.9198	4.1264	5.4043	6.4336	7.3190

Table 16 Effect of degree of orthotropy of individual layers on the fundamental frequency of simply-supported antisymmetric square laminates: $a/h=5$, $\bar{w}=10\times w(\rho h^2/E_T)^{1/2}$

Number of layers	Source	E_L/E_T				
		3	10	20	30	40
2	Exact	2.5031	2.7938	3.0698	3.2705	3.4250
	GTTR	2.4936	2.8011	3.1331	3.4060	3.6384
	STTR	2.4868	2.7955	3.1284	3.4020	3.6348
	FSDT	2.4834	2.7757	3.0824	3.3285	3.5333
	CLPT	2.7082	3.0968	3.5422	3.9335	4.2884
4	Exact	2.6182	3.2578	3.7622	4.0660	4.2719
	GTTR	2.6080	3.2863	3.8583	4.2208	4.4747
	STTR	2.6003	3.2782	3.8506	4.2139	4.4686
	FSDT	2.6017	3.2898	3.8754	4.2479	4.5083
	CLPT	2.8676	3.8877	4.9907	5.8900	6.6690
6	Exact	2.6440	3.3657	3.9359	4.2783	4.5091
	GTTR	2.6299	3.3700	3.9745	4.3483	4.6060
	STTR	2.6223	3.3621	3.9672	4.3419	4.6005
	FSDT	2.6228	3.3673	3.9771	4.3531	4.6106
	CLPT	2.8966	4.0215	5.2234	6.1963	7.0359
10	Exact	2.6583	3.4250	4.0337	4.4011	4.6498
	GTTR	2.6413	3.4128	4.0339	4.4140	4.6745
	STTR	2.6337	3.4051	4.0270	4.4079	4.6692
	FSDT	2.6335	3.4053	4.0255	4.4023	4.6577
	CLPT	2.9115	4.0888	5.3397	6.3489	7.2184

center of an edge ($x/a=0$, $y/b=0.5$, $z/h=0$). For deflections, GTTR gives the best results. STTR and FSDT values are almost the same, while CLPT values are least accurate. The error in the values predicted by CLPT also increases as the plate thickness increases. For the normal stresses σ_x and σ_y, the values given by GTTR and STTR are almost the same, both being very close to the exact value. FSDT values are slightly worse, but still quite good. For shear stress τ_{xz}, GTTR gives the best results, followed by STTR. FSDT values are not good, while CLPT values are uniformly zero since it does not take into account efects of shear deformation.

In Table 11, the transverse deflection w, and stresses σ_x, σ_y and τ_{xz} are given for a square three-ply laminate with the top and bottom plies being of equal thickness and made up of identical material ($h/a=0.1$, $h_1/h=0.1$, $h_2/h=0.8$, $h_3/h=0.1$). The modular ratio between the middle ply and the outer plies ($\beta=E_{x1}/E_{x2}$) is 10. The deflections and stresses are calculated at the same points as in Tables 7-10. Additionally, the variation of the stresses through the thickness of the plate is shown. For deflection, GTTR and STTR give the most accurate results. For normal stresses, the values predicted by GTTR and STTR are quie close to the exact values. For shear stress τ_{xz}, while the GTTR and STTR values are good at the mid-strface they do not compare very well with the exact solutions at the interfaces. This is because the stress values have been evaluated from the constitutive equations, and not from the equilibrium equations. FSDT, of course, predicts a constant

Table 17 Center deflections $\bar{w}$ of simply-supported [0/90] antisymmetric cross-ply square laminates under different load and boundary conditions: h/a=0.2, $\bar{w}=w\times 10^4$

Load	Source	Type of solution	Boundary condition					
			SSSS	SSCC	SSFF	SSCS	SSCF	SSSF
UL	GTOT	FEM_Q	243.655	147.232	497.658	187.363	291.309	378.458
		FEM_L	241.441	145.831	489.388	185.587	287.518	373,461
	GTTR	Exact	242.360	143.948	502.516	184.167	291.594	380.854
		FEM	241.683	138.282	487.221	180.770	281.506	372.645
	STTR	Exact	244.985	143.898	504.345	185.312	292.214	385.189
		FEM	246.618	142.555	505.993	185.535	292.367	384.487
	FSDT	Exact	251.648	157.041	517.696	196.610	305.935	392.673
		FEM_Q	251.786	157.191	517.809	196.902	306.269	392.848
		FEM_L	251.774	157.213	515.218	196.891	305.502	391.586
	CLPT	Exact	186.061	73.5713	406.464	116.205	206.741	303.552
		FEM	185.810	73.0552	405.772	115.758	206.158	303.089
LL	GTOT	FEM_Q	42.8409	27.6154	82.6797	33.9589	50.2569	63.9855
		FEM_L	42.6595	27.5168	81.6657	33.8195	49.8467	63.4303
	GTTR	Exact	41.7723	26.2295	82.4316	32.6589	49.7416	63.7339
		FEM	42.3626	26.1251	80.8925	32.8030	48.6096	62.9167
	STTR	Exact	42.7476	26.7977	83.4949	33.6698	50.4841	64.4209
		FEM	43.1342	26.7958	83.8756	33.5496	50.3330	64.7923
	FSDT	Exact	44.4738	29.5071	86.2330	35.9912	53.1823	66.6447
		FEM_Q	45.4636	30.5325	87.3179	36.8064	54.0150	67.6512
		FEM_L	45.5128	30.5473	87.0559	36.8320	53.9582	67.5559
	CLPT	Exact	30.4292	12.7364	65.0200	19.4449	33.6513	48.8696
		FEM	30.3186	12.6468	64.8752	19.3421	33.5469	48.7445

shear stress state through the thickness of the plate.

3.2.2. Natural vibration result

Tables 12, 13 and 14 give the natural frequencies of the first three antisymmetric modes of free vibration of a homogeneous plate. GTTR gives the best results, followed closely by STTR and FSDT. Tables 15 and 16 give the fundamenatal frequencies of free vibration for symmetric and antisymmetric cross-ply plates. The plates have different number of layers, and varying degrees of orthotropy of individual layers, ie., different values of E_l/E_t, Here E_l refers to the modulus in the longitudinal (fiber) direction, and E_t refers to the modulus in the transverse direction. In most cases, GTTR gives the most accurate results. However for N=3 in the case of symmetric plates, and N=2 in the case of antisymmetric plates, FSDT gives the best results; CLPT consistently overpredicts the frequency values.

3.3. FEM results vs. analytical solutions

3.3.1. Static analysis

Here the finite element results are compared with the analytical solutions of laminate

Table 18 Center deflections $\bar{w}$ of simply-supported [0/90/0] symmetric cross-ply square laminates under different load and boundary conditions: h/a=0.2, $\bar{w}=w\times 10^4$

Load	Source	Type of solution	Boundary condition					
			SSSS	SSCC	SSFF	SSCS	SSCF	SSSF
UL	GTOT	FEM_Q	185.576	126.286	981.749	153.417	358.479	577.123
		FEM_L	184.718	135.832	952.044	152.762	353.641	565.342
	GTTR	Exact	185.282	120.408	981.805	149.429	352.065	577.725
		FEM	185.396	119.594	964.767	148.920	348.281	570.598
	STTR	Exact	188.344	120.849	997.597	150.832	356.288	586.641
		FEM	188.414	119.588	996.497	149.997	354.453	585.318
	FSDT	Exact	182.011	126.505	995.718	152.194	359.601	583.509
		FEM_Q	182.148	126.638	995.841	152.330	359.742	583.641
		FEM_L	182.500	127.093	990.293	152.738	359.741	581.745
	CLPT	Exact	96.6214	22.4279	874.983	43.6137	190.336	480.104
		FEM	96.6326	22.4389	874.994	43.6248	190.347	480.116
LL	GTOT	FEM_Q	34.9732	25.5374	160.186	29.8621	62.1453	96.5535
		FEM_L	34.8992	25.5056	155.932	29.8081	61.5151	94.9372
	GTTR	Exact	34.6047	24.2636	159.889	28.8045	60.8068	96.3339
		FEM	34.8516	24.4359	157.473	29.0929	60.5043	95.4652
	STTR	Exact	35.7848	25.0037	163.097	29.8045	62.1693	98.4478
		FEM	36.2897	25.3514	163.469	30.1974	62.4380	98.7609
	FSDT	Exact	34.8615	26.0017	162.883	30.1100	62.7846	98.0323
		FEM_Q	36.0259	27.1659	164.142	31.2744	63.9944	99.2413
		FEM_L	36.0608	27.2026	163.584	31.3098	64.0350	99.0880
	CLPT	Exact	17.5725	5.39766	139.939	8.98087	320.882	77.8618
		FEM	17.5800	5.44122	139.973	9.01349	321.435	77.8826

theories. The analytical and finite element solutions for center deflections w and normal stress σ_x in [0/90] [0/90/0] square laminates are presented in Tables 17-19. The solutions are evaluated using the different theories, under different boundary and loading conditions. The dimensions of the laminate are taken to be 10 inch $\times$ 10 inch, and results are presented for h/a =0.2. The material is graphite-epoxy (see Table 1 for properties). Two different loading conditions are considered: a uniformly distributed load (UL) over the entire plate, and a line load (LL) along the centerline of the plate parallel to the x-axis. The magnitude of the loads are 1000 lb/sq.in. for UL and 1000 lb/in. for LL. The elements and discretizations used have been explained earlier.

For both deflections and normal stresses, GTTR and GTOT give the best results followed closely by STTR. FSDT gives good results for transverse deflections even in the case of thick plates, but its values for normal stresses in thick plates are not very good. As is well documented, CLPT does not give good results in the case of thick plates for either w or σ_x. Due to the fine discretization employed, the finite element solutions are very close to the analytical solutions for each theory.

Nondimensional center deflections, $\bar{w}$, ($\bar{w}=100wh^3E_2/a^4q_0$), and nondimensional center normal stresses, $\bar{\sigma}_x$, ($\bar{\sigma}_x=10\sigma_x h^2/a^2q_0$) are plotted against different parameters like span-to-thickness ratio (a/h), aspect ratio (b/a), and degree of orthotropy (E_1/E_2), for different stacking sequences, number of layers, boundary conditions, and using the different theories. The σ_x

Table 19 Center normal stresses $\bar{\sigma}_x$ for simply-supported [0/90/0] symmetric cross-ply square laminates under different load and boundary conditions: h/a=0.2, $\bar{\sigma}_x=\sigma_x/10$

Load	Source	Type of solution	Boundary condition					
			SSSS	SSCC	SSFF	SSCS	SSCF	SSSF
UL	GTOT	FEM_Q	973.641	320.041	30.2642	653.548	256.610	459.610
		FEM_L	960.459	314.217	31.6600	647.906	241.614	450.267
	GTTR	Exact	992.114	334.057	30.8988	639.800	308.397	278.964
		FEM	982.709	327.325	19.4407	644.871	274.358	462.694
	STTR	Exact	995.369	334.509	17.6550	635.385	327.724	473.740
		FEM	995.066	343.802	17.9696	647.690	291.056	469.563
	FSDT	Exact	1085.14	431.937	20.2023	733.613	262.910	516.305
		FEM_Q	1079.65	427.733	20.2709	751.250	209.910	499.454
		FEM_L	1072.81	424.712	20.6861	750.503	200.040	493.030
	CLPT	Exact	1208.39	464.315	32.3017	680.166	280.892	629.531
		FEM	120.931	465.612	32.7585	690.654	259.913	627.118
LL	GTOT	FEM_Q	172.668	58.9037	8.97681	117.795	33.9851	83.3899
		FEM_L	170.031	57.6618	9.07930	116.507	32.0467	81.5028
	GTTR	Exact	176.810	62.2996	6.07885	116.326	43.2240	86.1107
		FEM	174.505	61.3136	6.07714	117.201	36.8403	83.7726
	STTR	Exact	178.970	67.9291	6.66829	118.186	43.1874	87.4451
		FEM	181.575	70.8969	8.91552	123.380	34.8713	88.8165
	FSDT	Exact	195.984	82.6924	7.51739	135.614	32.2051	95.7561
		FEM_Q	194.187	81.5802	7.61716	138.217	24.3347	91.8081
		FEM_L	191.814	80.2266	7.53731	137.054	23.4689	90.0119
	CLPT	Exact	217.132	107.570	11.6526	137.876	23.9371	115.618
		FEM	218.384	109.158	12.8193	140.920	19.7495	115.979

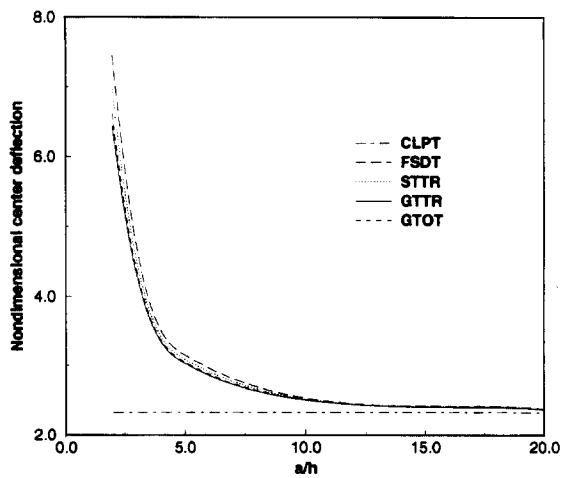

Fig. 2 Nondimensional center deflection $\bar{w}$ vs span-to-thickness ratio a/h for [0/90] square SSSS laminate using different theories

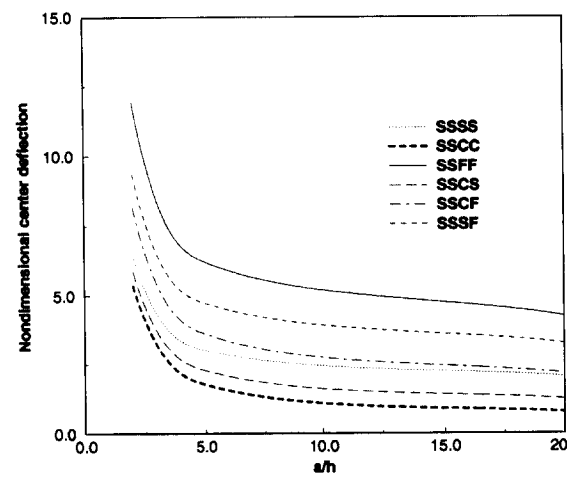

Fig. 3 Nondimensional center deflection $\bar{w}$ vs span-to-thickness ratio a/h for [0/90] square laminate with different boundary conditions using GTTR

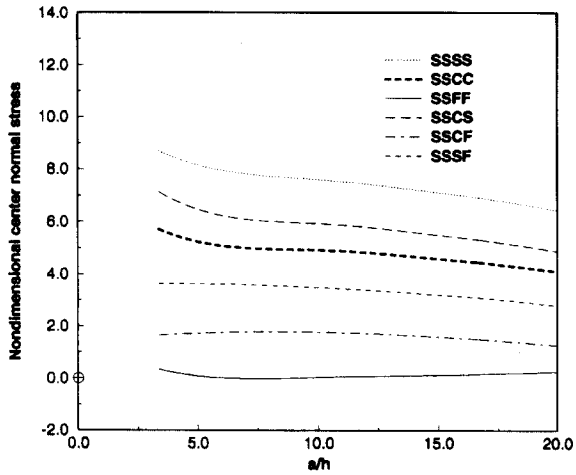

Fig. 4 Nondimensional center normal stress $\overline{\sigma}_x$ vs span-to-thickness ratio a/h for a [0/90] square laminate with different boundary conditions using GTTR

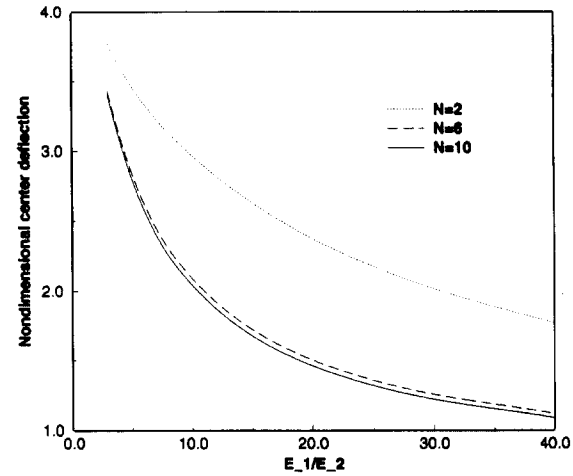

Fig. 5 Nondimensional center deflection $\overline{w}$ vs modular ratio E_1/E_2 for antisymmetric cross-ply square SSSS laminates (a/h=5) with different number of layers N using GTTR

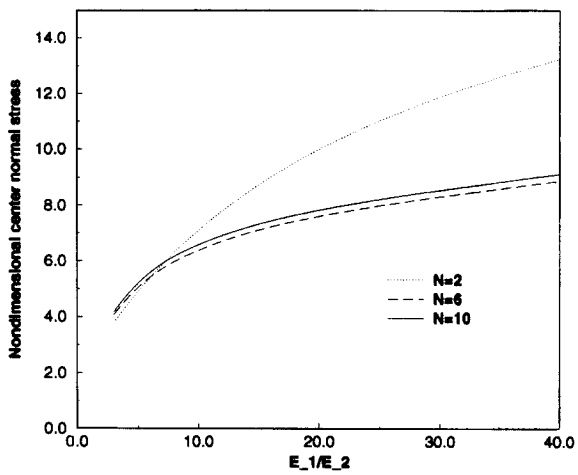

Fig. 6 Nondimensional center normal stress $\overline{w}$ vs modular ratio E_1/E_2 for antisymmetric cross-ply SSSS laminates (a/h=5) with different number of layers N using GTTR

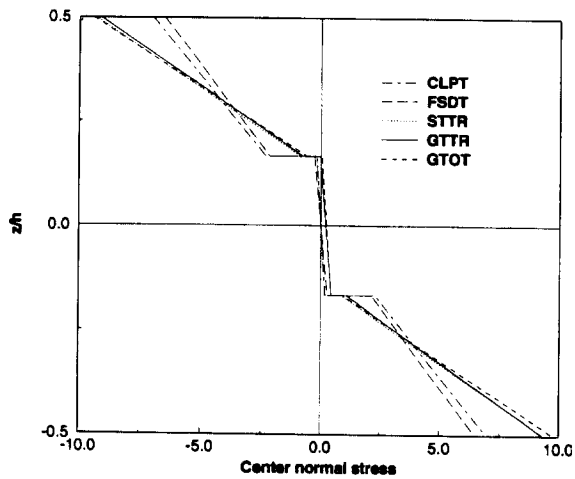

Fig. 7 Variation of center normal stress σ_x/q_0 through the thickness of a [0/90/0] square SSCC laminate using different theories

stress has been taken to be at the center of the top layer of the laminate. In all examples, the load is an uniformly distributed transverse load over the entire plate (UL). Unless mentioned otherwise, the material is graphite-epoxy.

In Fig. 2, $\overline{w}$ has been plotted against the span-to-thickness ratio, a/h, for a [0/90] square laminate with SSSS boundary condition. For CLPT $\overline{w}$ remains constant with a/h. All other theories give very close results for $\overline{w}$. In Figs. 3 and 4, $\overline{w}$ and $\overline{\sigma}_x$ have been plotted against a/h for a square [0/90] laminate using GTTR for different boundary conditions. The

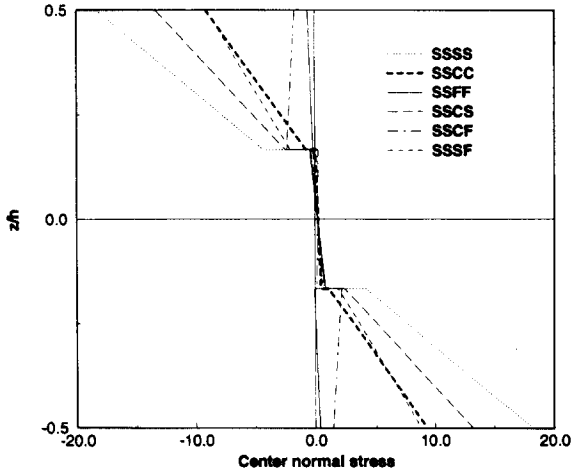

Fig. 8 Variation of center normal stress σ_x/q_0 through the thickness of a [0/90/0] square laminate for different boundary conditions using GTTR

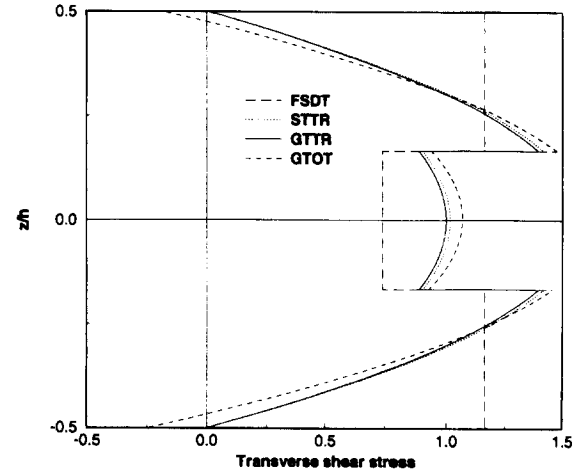

Fig. 9 Variation of transverse shear stress τ_{xz}/q_0 through the thickness of a [0/90/0] square SSSS laminate using different theories

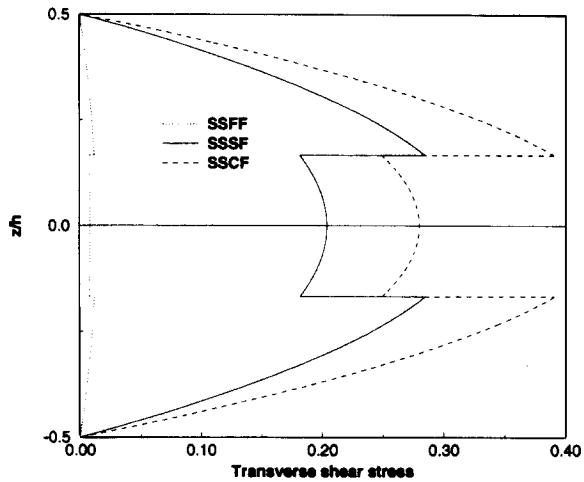

Fig. 10 Variation of transverse shear stress τ_{xz}/q_0 through the thickness of a [0/90/0] square laminate for different boundary conditions (SSFF, SSSF, SSCF) using GTTR

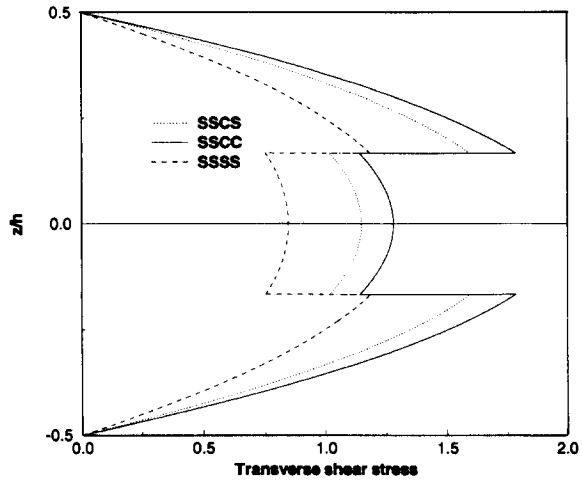

Fig. 11 Variation of transverse shear thress τ_{xz}/q_0 through the thickness of a [0/90/0] square laminate for different boundary conditions (SSCS, SSCC, SSSS) using GTTR

deflections are lowest for SSCC laminates, and highest for SSFF laminates. The normal stresses are highest for SSSS laminates, and lowest for SSFF laminates.

In Figs. 5 and 6, $\overline{w}$ and $\overline{\sigma}_x$ have been plotted against the modular ratio, E_1/E_2, for a square SSSS antisymmetric cross-ply laminate with a/h=5. The number of layers considered are N=2, 6 and 10. The material considered is Material 3 in Table 1. $\overline{w}$ decreases with increasing modular ratio, and it decreases with increasing number of layers. This trend, again, was observed for symmetric cross-ply laminates in Fig. 2. However, in this case, for an

Table 20 Dimensionless fundamental frequencies of simply-supported antisymmetric cross-ply square laminates under different boundary conditions: $\bar{w}=(wb^2/h)(\rho/E_2)^{1/2}$

No. of layers	h/a	Source	Boundary condition					
			SSSS	SSCC	SSFF	SSCS	SSCF	SSSF
2	0.2	GTTR	9.0959	11.8688	6.1937	10.5642	7.1390	6.3710
		STTR	9.0874	11.8906	6.1277	10.3934	6.8354	6.3876
		FSDT	8.8335	10.8964	5.9518	9.8223	6.6383	6.2125
		CLPT	10.7207	17.7407	7.1236	13.6273	8.0412	7.4501
	0.4	GTTR	6.5792	8.1060	4.6286	7.1105	5.0883	4.7419
		STTR	6.5729	7.8813	4.5655	7.1347	5.0754	4.7234
		FSDT	6.1204	6.6426	4.2426	6.3267	4.7071	4.4088
		CLPT	9.3590	15.2460	5.4890	11.7556	7.3849	5.7556
10	0.2	GTTR	11.6861	13.9043	8.1804	12.7862	8.9620	8.2357
		STTR	11.6730	13.5673	8.1553	12.5137	8.9664	8.2877
		FSDT	11.6446	12.9229	8.1385	12.1967	8.9189	8.2641
		CLPT	12.1671	30.8537	11.4586	23.3477	13.6183	11.8152
	0.4	GTTR	7.1302	8.3201	5.4638	7.9060	5.7058	5.1159
		STTR	7.1237	8.1133	5.3268	7.5335	5.6044	5.1061
		FSDT	6.9550	7.1736	5.1617	7.0083	5.4273	4.9807
		CLPT	16.5306	27.0606	12.7885	18.7728	13.0223	12.1574

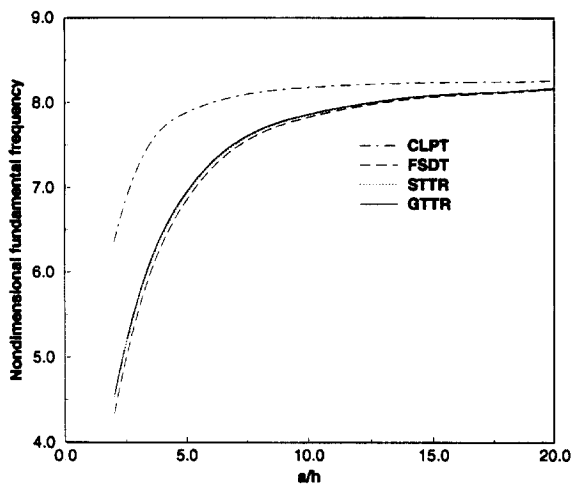

Fig. 12 Nondimensional fundamental frequency $\bar{w}$ vs span-to-thickness ratio a/h for [0/90] square SSSS laminate using different theories

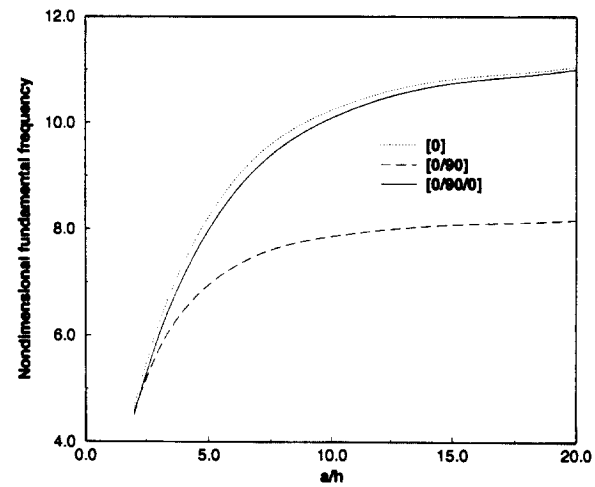

Fig. 13 Nondimensional fundamental frequency $\bar{w}$ vs span-to-thickness ratio a/h for different layups of a square SSCS laminate using GTTR

antisymmetric cross-ply laminate, the difference in deflections between N=2 and N=6 is quite substantial due to the bending-stretching coupling present for the layer case. The normal stresses increase with increase in modular ratio; they are the highest for N=2 and significantly lower for N=6 and N=10.

In the remaining figures discussed here, the span-to-thickness ratio, a/h, is taken as 5. Fig. 7

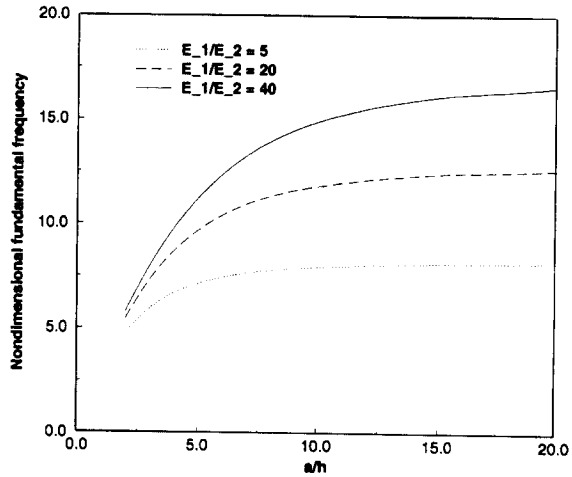

Fig. 14 Nondimensional fundamental frequency $\overline{w}$ vs span-to-thickness ratio a/h for [0/90/0] square SSSS laminate with different modular ratios using GTTR

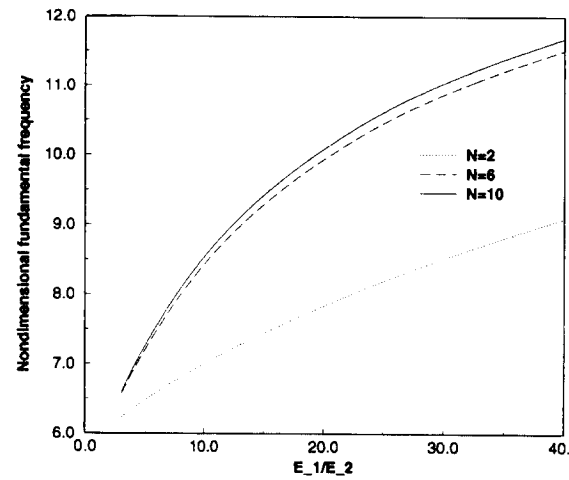

Fig. 15 Nondimensional fundamental frequency $\overline{w}$ vs modular ratio E_1/E_2 for antisymmetric cross-ply square SSSS laminates (a/h=5) with different number of layers N using GTTR

gives the variation of σ_x stress through the thickness of a [0/90/0] SSCC laminate. The stresses have been evaluated at the center of the plate (x/a=0.5, y/b=0.5). The 0 degree plies carry the most load compared to the 90 degree ply. Fig. 8 gives the variation of σ_x stress through the thickness of a [0/90/0] laminate using GTTR for different boundary conditions. The values are highest in magnitude for SSSS and lowest for SSFF, with the other boundary conditions falling in between.

Fig. 9 gives the variation of τ_{xz} stress through the thickness of a [0/90/0] SSSS laminate. The τ_{xz} stresses have been evaluated at the same location as the τ_{xy} stresses, at (x/a=0.75, y/b= 0.75). The variation in magnitude is less in the 90 degree ply compared to the 0 degree ply. STTR, GTTR and GTOT correctly predict the quadratic variation within each layer, whereas FSDT gives constant values in each layer. Figs. 10 and 11 give the variation of τ_{xz} stress through the thickness of a [0/90/0] laminate using GTTR for different boundary conditions. Note that the scales used for τ_{xz} are different for the two graphs. The laminates involving free boundary conditions have much lower stress values than the rest.

3.3.2. Free vibration analysis

Results of free vibration analysis are presented in this section. The dimension of the plate is the same as in static analysis, and the material properties are those of graphite-epoxy unless otherwise mentioned. Table 20 gives the lowest natural frequency of vibration of antisymmetric square plates under different boundary conditions.

In Fig. 12, the nondimensional fundamental frequency, $\overline{w}$, ($\overline{w}=w(\rho a^4/E_2h^2)^{1/2}$) is plotted against a/h for square SSSS [0/90] laminates. Apart from CLPT, which gives consistently higher values, all the other theories give quite close results. A plot of $\overline{w}$ versus a/h is shown in Fig. 13 for three different layups [0], [0/90], and [0/90/0], of square SSCC laminates. The laminate [0/90] has the lowest frequency among the three. The frequencies of [0] and [0/90/0]

laminates are very close.

For Figs. 14 and 15, the material properties are those of Material 3 in Table 1. In Fig. 14, $\overline{w}$ is plotted against a/h for a square [0/90/0/90] SSSS laminate for different modular ratios E_1/E_2. The frequencies are lowest for E_1/E_2=5, and increases with increasing modular ratio. In Fig. 15, $\overline{w}$ is plotted against E_1/E_2 for square antisymmetric cross-ply SSSS laminates with a/h=5 using GTTR. $\overline{w}$ reaches an upper limit with increase in the number of layers N, and also increases with increase in modular ratio, trends which were also evident in the last two plots.

4. Conclusions

The inability of CLPT to model thick plates is well known. Since thick plates have been considered in most of the numerical examples, that shortcoming of CLPT is well evident. It gives lower values for deflections, and higher values for frequencies. It gives higher values for some stresses, and lower values for some others. FSDT gives reasonably good results for deflections and frequencies, even for thick plates. But the error in the inplane stress values predicted by FSDT increases as the plate gets thicker. The transverse shear stress values given by FSDT are quite inaccurate for all thicknesses. GTTR and GTOT give the most accurate results in almost every case. GTTR has the added advantage that it takes into account the zero transverse shear stress conditions at the top and bottom of the plate. Overall, the STTR values are always very close to those predicted by GTTR and GTOT. Considering the fact that getting solutions using STTR requires less computational effort than doing the same using GTTR and GTOT, STTR seems to possess the optimal performance among the ESL theories considered in this study.

Acknowledgements

The support of this work through the Oscar S. Wyatt Chair is gratefully acknowledged.

References

Bose, P. (1995), "An evaluation of classical and refined equivalent-single-layer laminate theories", M.S. Thesis, Virginia Polytechnic Institute & State University, Blacksdurg, VA.

Bose, P. and Reddy, J.N. (1998), "Analysis of composite plates using various plate theories. Part 1: Formulation and analytical solutions", *Structural Engineering and Mechanics, An Int. J.* **6**(6), 583-612.

Reddy, J.N. (1993), *An Introduction to the Finite Element Method*, McGraw-Hill, 2nd edition.

Reddy, J.N. (1997), *Mechanics of Laminated Plates: Theory and Analysis*, CRC Press, Boca Raton, FL.

Srinivas, S., Rao, A.K. and Joga Rao, C.V. (1966), "Flexure of simply supported thick homogeneous and laminated rectangular plates", *Zeitschrift fur Angewandte Mathematik and Mechanik,* **49**, 449-458.

Srinivas, S. and Rao, A.K. (1970), "Bending, vibrations and buckling of simply supported thick orthotropic rectangular plates and laminates", *International Journal of Solids and Structures,* **6**, 1464-1481.

Srinivas, S., Joga Rao, C.V. and Rao, A.K. (1970), "An exact analysis for vibration of simply-

supported homogeneous and laminated thick rectangular plates", *Journal of Sound and Vibration,* **12**, 187-199.

Srinivas, S. (1973), "A refined analysis of composite laminates", *Journal of Sound and Vibration,* **30**, 495-507.

Noor, A.K. and Burton W. Scott, (1989), "Three-dimensional solutions for antisymmetrically laminated anisotropic plates", *Journal of Applied Mechanics, Trans. ASME,* 1-7.